*Int. J. Electrochem. Sci.*, 6 **(2011)** 3938 - 3950

International Journal of
ELECTROCHEMICAL
SCIENCE
www.electrochemsci.org

# Enhanced Photoelectrochemical Performance of Dye-Sensitized Solar Cells base on Iodine-PEDOT Composited Film

*Tsung-Hsuan Tsai, Shr-Chiang Chiou, Shen-Ming Chen*[*]*, Kuo-Chiang Lin*

Electroanalysis and Bioelectrochemistry Lab, Department of Chemical Engineering and Biotechnology, National Taipei University of Technology, No.1, Section 3, Chung-Hsiao East Road, Taipei 106, Taiwan (ROC).
[*]E-mail: smchen78@ms15.hinet.net

*Received:* 26 June 2011 / *Accepted:* 30 July 2011 / *Published:* 1 September 2011

Nanostructured iodine films with control the thickness which from 0- to 100- sweep-segments successfully electrodeposited on PEDOT/ITO glass substrates using the cyclic voltammetry (CV) method at room temperature. The formation mechanism of the iodine-PEDOT film is monitored by CV techniques, *UV-visible* spectroscopy, alternating current (AC) impedance spectroscopy, scanning electron microscopy (SEM) and atomic force microscopy (AFM). CV and AC impedance spectroscopy reveal that the iodine-PEDOT CEs have higher electrocatalytic activity for the $I_3^-/I^-$ redox reaction and a smaller charge transfer resistance than the PEDOT electrodes. It is found that iodine-PEDOT increased the reactive interface, which supports charge transfer at the interface. With an optimum iodine film thickness of 50 sweep-segments on PEODT CEs, a 19.5% improvement in the cell efficiency (from 4.1 to 19.5%) is achieved.

**Keywords:** Dye-sensitized solar cells, Iodine, PEDOT, N719 dye, Cyclic voltammetry, Photoelectrochemistry, EIS, AC impedance.

## 1. INTRODUCTION

Dye-sensitized solar cells (DSSCs) have attracted considerable attention due to their low production cost and relatively high energy conversion efficiency [1-3]. DSSCs consist of a dye-sensitized mesoporous $TiO_2$ film interpenetrated by a liquid electrolyte containing an iodine/iodide redox couple [4-7]. In order to further improve the performances of DSSCs, extensive efforts are on-going for each of its constituent components including nanocrystalline semiconductors [8], dye molecules [9], electrolytes [10] and counter electrodes (CEs) [11, 12].

Among constituent components in DSSCs, the function of counter electrode is the electron

transfer from the external circuit back to the redox electrolyte and catalyzing the reduction of the triiodide ion ($I_3^-$) [11]. Generally, platinum-coated transparent conductive oxide electrode is used as a counter electrode due to its excellent electrocatalytic activity for the $I_3^-/I^-$ redox couple. However, platinum is a noble metal and relatively expensive. Therefore, the cost of the platinum counter electrode represents more than 40% of the whole DSSC cell cost regardless of its preparation method. Furthermore, the slow dissolution of platinum counter electrode in the corrosive $I_3^-/I^-$ redox electrolyte deteriorates the long term stabilities of DSSCs [12].

Poly(3,4-ethylenedioxythiophene) (PEDOT) has been widely investigated as an electronically conducting polymer. It can be easily electrodeposited onto a surface by the electrooxidation of its monomer [13–19].

A PEDOT film in its oxidized form has been found to have high conductivity and stability at physiological pH [20, 21]. Recently, the PEDOT film always cooperated with other material as the counter electrode used in DSSCs, such as graphene-PEDOT-PSS [22], *f*-MWCNT-PEDOT [23], PEDOT-PSS [24-26] and PEDOT-PSS-Pt [27]. However, the PEDOT film can be an efficient mediator and enhance the efficiency of DSSC.

Redox mediators are small electroactive compounds that effectively shuttle electrons between the analyte and electrode. Iodine is an indispensable element to life and more research has focused on the oxidation of iodide ion and the reduction of iodine on electrodes to achieve the quantitative determination of iodine [16]. Regarding the behavior of iodide ion as a mediator, the electrochemical oxidation of iodide ion is oxidized to iodine, and the iodine then reacts in a chemical reaction [16, 28-34].

In this work, the reaction of iodine (electrogenerated from iodide ion by CV) which based on PEDOT modified ITO electrode was used for the counter electrode of DSSC. The effects of CV sweep-segments (S.S.) on electrode characteristics and surface morphology were investigated by SEM and AFM.

Different sweep-segments of iodine modified on PEDOT/ITO were studied by UV-Vis. It was observed that iodine-PEDOT/ITO successfully used as a counter electrode and significantly influenced the performance of DSSCs. The photovoltaic performances of the devices were analyzed.

## 2. EXPERIMENTAL

### *2.1 Materials and chemicals*

3,4-ethylenedioxythiophene (EDOT), P25 $TiO_2$ powder, N719 dye, 4-t-butylpyridine (TBP), Triton X-100 solution and PEG 20000 were purchased from Sigma-Aldrich (USA). Indium tin oxide (ITO) (7 $\Omega \cdot cm^{-2}$) was purchased from Merck Display Technologies (MDT) Ltd (Taiwan). Lithium iodide (LiI, analytical grade), Potassium iodide and iodine ($I_2$, analytical grade) were obtained from Wako (Japan). 60 μm thick surlyn films were purchased from Solaronix S.A., Aubonne, (Switzerland). Double distilled deionized water (DDDW) was used to prepare all the solutions.

*2.2. Apparatus*

All electrochemical experiments were performed using a CHI 750a potentiostat (CH Instruments, USA). Electrochemical impedance studies (EIS) were performed using a ZAHNER impedance analyzer (Germany). UV–visible spectra were obtained using Hitachi U-3300 spectrophotometer (Japan). The atomic force microscope (AFM) images were recorded using a multimode scanning probe microscope (Being Nano-Instruments CSPM-4000, China). Field emission scanning electron microscope (FE-SEM) images were recorded using a HITACHI S-4700 (Japan).

*2.3 Preparation of Photoanode and Photocathode*

9 g P25 $TiO_2$ powder with 0.1 ml Triton X-100, 1g PEG 20000 and 18 ml DDDW were mixed well in a dried agate mortar for one hour. The final mixture was stirred for an additional 2 days to obtain the desired $TiO_2$ paste. The above obtained $TiO_2$ paste solution was spin-coated on an ITO glass substrate at 1000 rpm for 10 s and 2000 rpm for 30 s. The formed film was annealed at 450 °C for 1 hour in atmosphere. The PEDOT modified glassy carbon electrodes (PEDOT/GCE) were prepared through the EDOT electropolymerization by cyclic voltammetry [14, 16, 20-21]. An ITO glass was ultrasonically washed with acetone and double-distilled water for 10 min acted as the working electrode in the three-electrode system (Pt wire auxiliary electrode and Ag/AgCl reference electrode) was immersed in the above solution. CV was carried out using a CHI750a electrochemical workstation (CH Instruments, USA) to electrodeposit iodine onto the PEDOT/ITO glass and various thicknesses of 0-, 10-, 20-, 50-, and 100-sweep-segments (S.S.) [35]. The PEDOT/ITO electrode was immersed in $1\times10^{-3}$ M potassium iodide solution overnight as an experimental control group (immersion-iodine-PEDOT/ITO). The above electrodes were separated by a 60 μm thick surlyn film and sealed together by heating. A thin layer of electrolyte was introduced into the inter electrode space. The electrolyte contains 0.1 M LiI, 0.05 M $I_2$, and 0.5 M 4-tertbutylpyridine (TBP) in dehydrated acetonitrile.

## 3. RESULTS AND DISCUSSION

*3.1 The micromorphology of iodine-PEDOT films*

Based on the different electrodeposit sweep-segments of iodine films onto PEDOT/ITO, the morphology of these films were studied by SEM. Fig. 1A shows a SEM micrograph of PEODT/ITO surface, the PEDOT/ITO surface provided a network structure surface. Fig. 1B shows 10-S.S. of iodine film modified on PEDOT/ITO surface of a network structure of 5 μm. The 20-, 50- and 100-S.S. of iodine film surface as shown in Fig. 1C, D and E, the electrode surface provide a diamond-like shape. Fig. 1F showed the PEDOT/ITO immersed in $1x10^{-3}$ M potassium iodide solution overnight and the iodine film was successfully adsorbed on PEDOT/GCE surface. Compared with the different sweep-segments of iodine films electrodeposit onto PEDOT/ITO surface (Fig. 1B, C, D and E), the morphology was totally different.

Fig. 2 showed the AFM images of different sweep-segments of iodine films onto PEDOT/ITO surface and furnished the comprehensive information. The AFM parameters have been evaluated for 1000×1000 nm surface area.

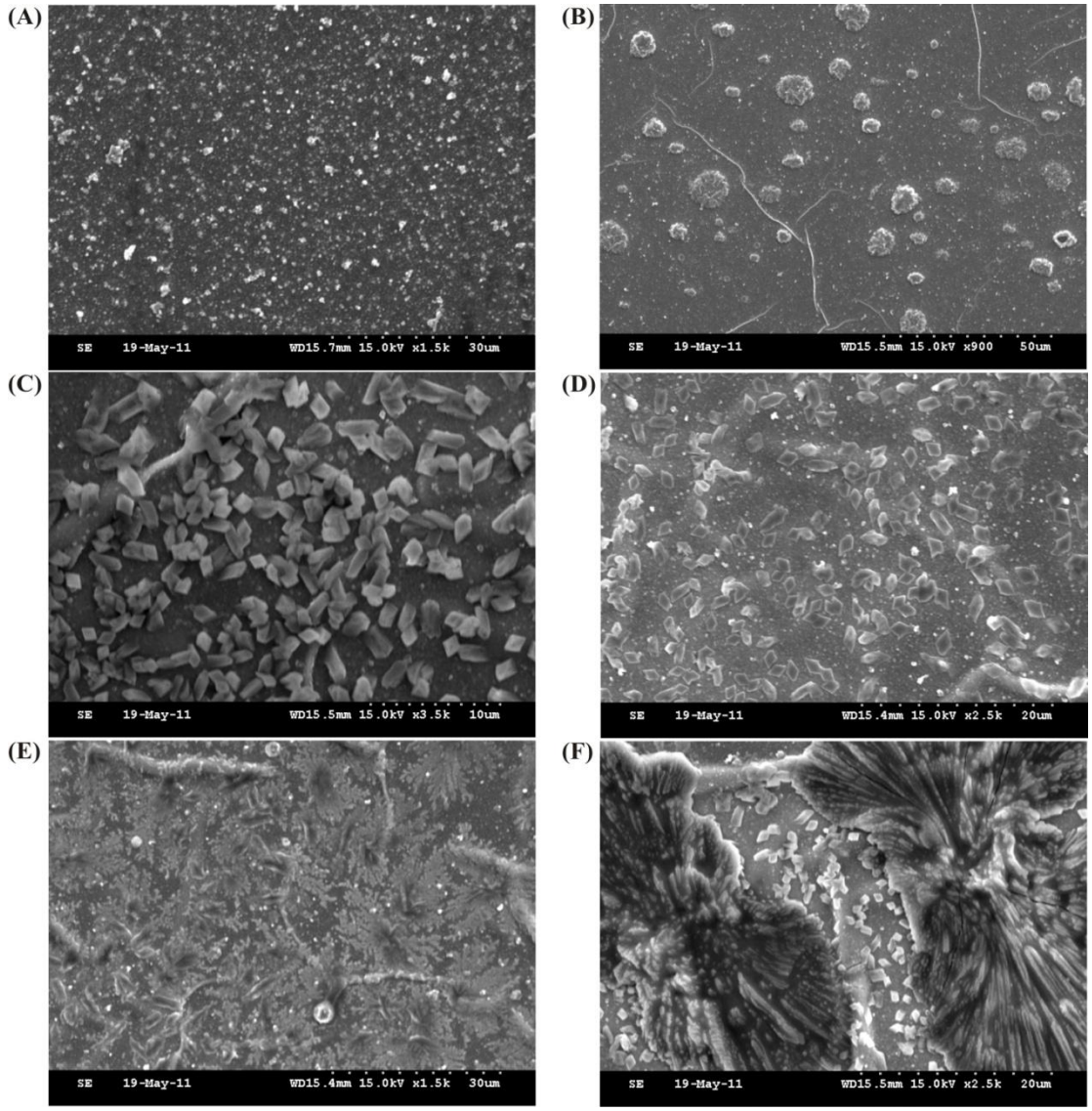


**Figure 1.** SEM images of **(A)** PEDOT/GCE, **(B)** 10-S.S. iodine-PEDOT/GCE, **(C)** 20-S.S. iodine-PEDOT/GCE, **(D)** 50-S.S. iodine-PEDOT/GCE, **(E)** 100-S.S. iodine-PEDOT/GCE, **(F)** immersion-iodine-PEDOT/GCE.

The surface morphology of iodine-PEDOT/ITO was examined by using the tapping mode. Figure 2 showed the 2D magnified view of (A) PEDOT/ITO, (B) 10-S.S. iodine-PEDOT/ITO, (C) 20-S.S. iodine-PEDOT/ITO, (D) 50-S.S. iodine-PEDOT/ITO, (E) 100-S.S. iodine-PEDOT/ITO and (F) immersion-iodine-PEDOT/ITO. From Figure 2, we can see the existence of iodine film in obvious manner with the average size range of (A) 30 to 50 nm, (B) 50 to 80 nm, (C) 50 to 90 nm, (D) 50 to 80 nm, (E) 80 to 120 nm and , (F) 100 to 120 nm. More importantly, the surface roughness factors ($R_a$) for

the PEDOT/ITO, the 10-S.S. iodine-PEDOT/ITO, the 20-S.S. iodine-PEDOT/ITO, the 50-S.S. iodine-PEDOT/ITO, the 100-S.S. iodine-PEDOT/ITO and immersion-iodine-PEDOT/ITO are 2.89, 33.9, 40.6, 56.3, 45.5 and 32.4 nm, respectively, as shown in Table 1.

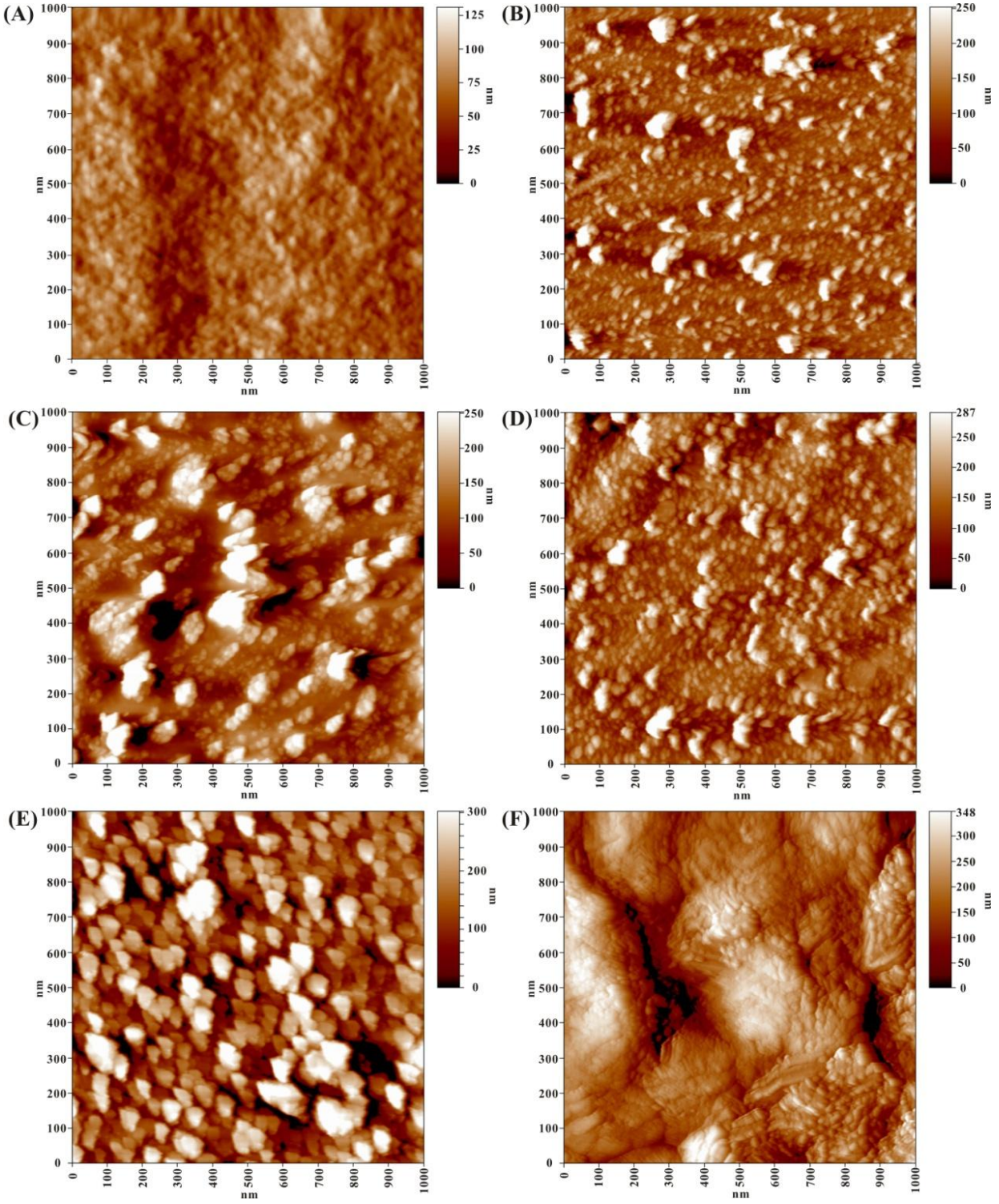


**Figure 2.** AFM images of **(A)** PEDOT/GCE, **(B)** 10-S.S. iodine-PEDOT/GCE, **(C)** 20-S.S. iodine-PEDOT/GCE, **(D)** 50-S.S. iodine-PEDOT/GCE, **(E)** 100-S.S. iodine-PEDOT/GCE, **(F)** immersion-iodine-PEDOT/GCE.

**Table 1.** Comparison surface roughness of different sweep-segments iodine film on PEDOT/ITO.

| Iodine | Parameters | | | |
|---|---|---|---|---|
| (sweep segments) | $R_a$ (nm) | RMS (nm) | Avg. hight (nm) | Avg. size (nm) |
| 0 | 2.89 | 6.95 | 4.30 | 47.97 |
| 10 | 33.9 | 40.8 | 42.28 | 82.86 |
| 20 | 40.6 | 58.2 | 58.30 | 81.9 |
| 50 | 56.3 | 71.6 | 56.05 | 78.57 |
| 100 | 45.5 | 52.4 | 38.75 | 88.41 |
| Immersion | 32.4 | 44.1 | 73.68 | 119.26 |

It is well known that more rough surface exhibits more catalytic reduction activity on the $I^-/I_3^-$ redox couples [16, 36]. From the above results, conducting polymer network structure provided a substrate for successful electrodeposit the iodine film onto the PEDOT/ITO surface.

*3.2 Transmittance spectra and XRD analysis with various CEs*

In this study, the iodine-PEDOT-CEs were prepared by electrodepositing iodine film on PEDOT/ITO substrates, and the electrodeposit sweep-segments were varied from 10 to 100.

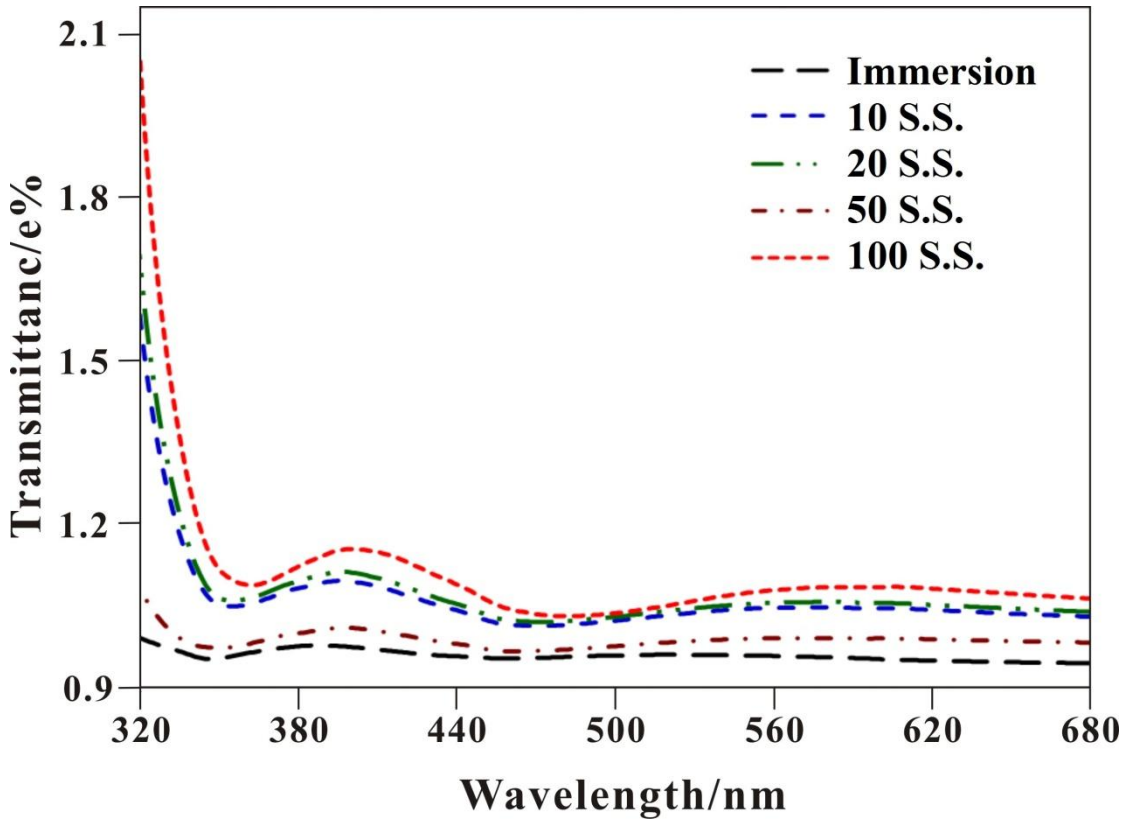


**Figure 3.**Typical UV–vis transmittance spectra of (A) immersion-iodine-PEDOT/ITO, (B) 10-, (C) 20-, (D) 50- and (E) 100-sweep segments iodine-PEDOT/ITO.

As shown in Fig. 3, the transmittance of iodine-PEDOT-CE increases with the sweep-segments of iodine in the range of 320 and 680 nm, except 50-sweep-segments. This might be the PEDOT modified electrode can determine iodide with good linear current response by cyclic voltammetry [16] and the 50-sweep-segments of iodine is the optimal condition for DSSC. Although high transparent iodine-PEDOT-CE is favorable for a back-illuminated DSSC, its catalytic ability is also to be taken into account from the viewpoint of efficiency of the cell.

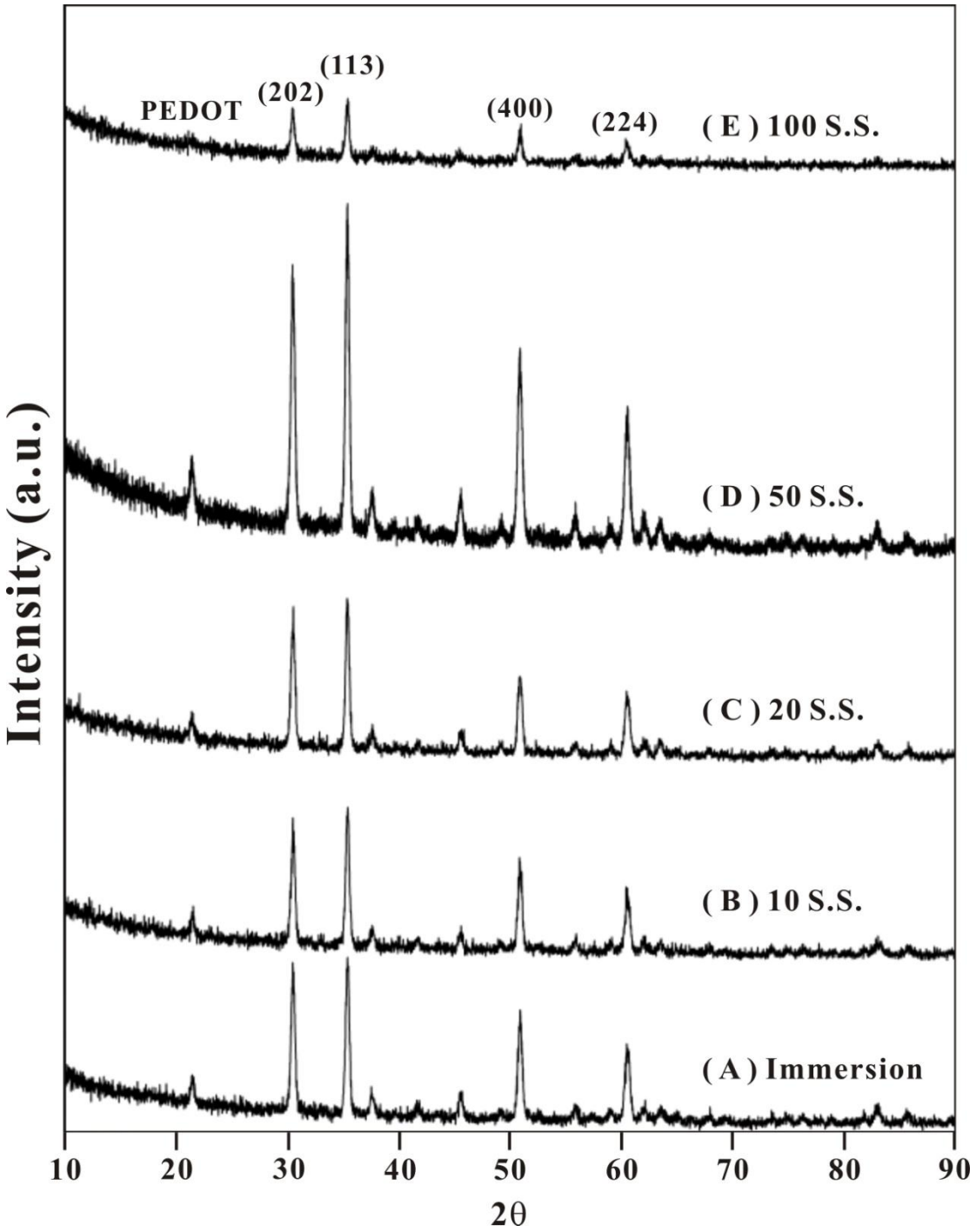


**Figure 4.** XRD spectra of (A) immersion-iodine-PEDOT/ITO, (B) 10-, (C) 20-, (D) 50- and (E) 100-sweep segments iodine-PEDOT/ITO.

The effect of different electrodeposited sweep-segment of iodine film modified on PEDOT/ITO was investigated using XRD and the results are shown in Fig. 4. Fig. 4A-E showed the XRD patterns of immersion-iodine-PEDOT/ITO, 10, 20, 50 and 100 sweep-segments iodine film modified on PEDOT/ITO. For iodine patterns, the peaks were found in 30.84°, 35.84°, 51.29° and 60.67° for (202), (113), (400) and (224). For PEDOT patterns, the peak was found in 21.44°, respectively. All these XRD peaks clearly validate the presence of iodine-PEDOT on the ITO surface.

### *3.3 Electrocatalytic activity for $I_3^-/I^-$ and $I_2/I_3^-$ with various CEs*

Fig. 5 showed the overlaid CVs recorded for various electrodeposition times of iodine on the PEDOT/ITO and the cathodic peak current ($I_{pc}$) of a CV represents the electrochemical activities.

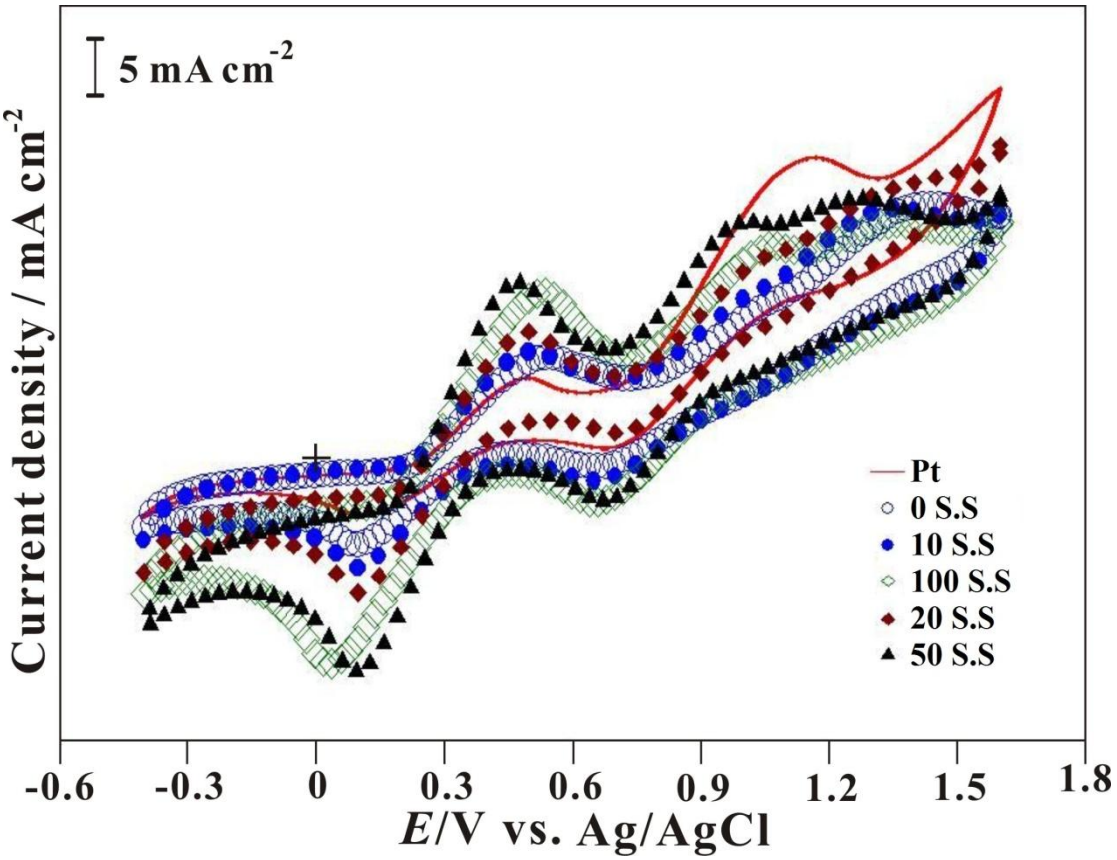


**Figure 5.** Cyclic voltammograms of electrodes based on Pt film and immersion, 0-, 10-, 20-, 50- and 100-sweep-segment (S.S.) iodine films on PEDOT/ITO, in an acetonitrile solution with 0.01 M LiI, 0.001 M $I_2$ and 0.1 M $LiClO_4$, initial E = + 1.6 V, high E = + 1.6 V, low E =−0.4 V, scan rate = 50 mV $s^{-1}$.

The absolute $I_{pc}$*'s* of the CVs showed increases with increasing deposition sweep-segments of iodine. These results suggest that the catalytic current of iodine-PEDOT layer for $I_3^-$ reduction increases with the increase of deposition sweep-segments. Compared with various iodine-

PEDOT/ITO, Pt/ITO and PEDOT/ITO, the bare ITO showed an $I_{pc}$ value close to zero, revealing that it has no catalytic current for the reduction of $I_3^-$. Two cathodic peaks of CV were represented the reduction reactions in redox reaction (1) and (2) [16].

$$I_3^- + 2e^- \rightarrow 3I^- \qquad (1)$$

$$3I_2 + 2e^- \rightarrow 2I_3^- \qquad (2)$$

This lack of reactivity is consistent with the poor photovoltaic performance of the DSSC. The reduction peaks of 10-200-sweepsegment iodine-PEDOT electrodes occurred in the range of 0 to +1.2 V (belonging to $I_3^- + 2e^- \rightarrow 3I^-$). The peak potential separations ($\Delta E_p$) of $I_3^-/I^-$ ($I_2/I_3^-$) for 0-, 10-, 20-, 50- and 100-sweep-segments iodine-PEDOT and Pt electrodes were 323 (104), 300 (103), 289 (105), 287 (97.1), 285 (101) and 301 mV (92.3 mV), respectively (Fig. 5). The $\Delta E_p$ (>>0.059 V/n, n = 2 for $I_3^-$, n = 2/3 for $I_2$) indicated that all of the above-mentioned electrode reactions were kinetically controlled and irreversible [35]. The lower $\Delta E_p$ of Pt and the 50-sweep-segment iodine film indicated that they were more electrochemically active relative to the others.

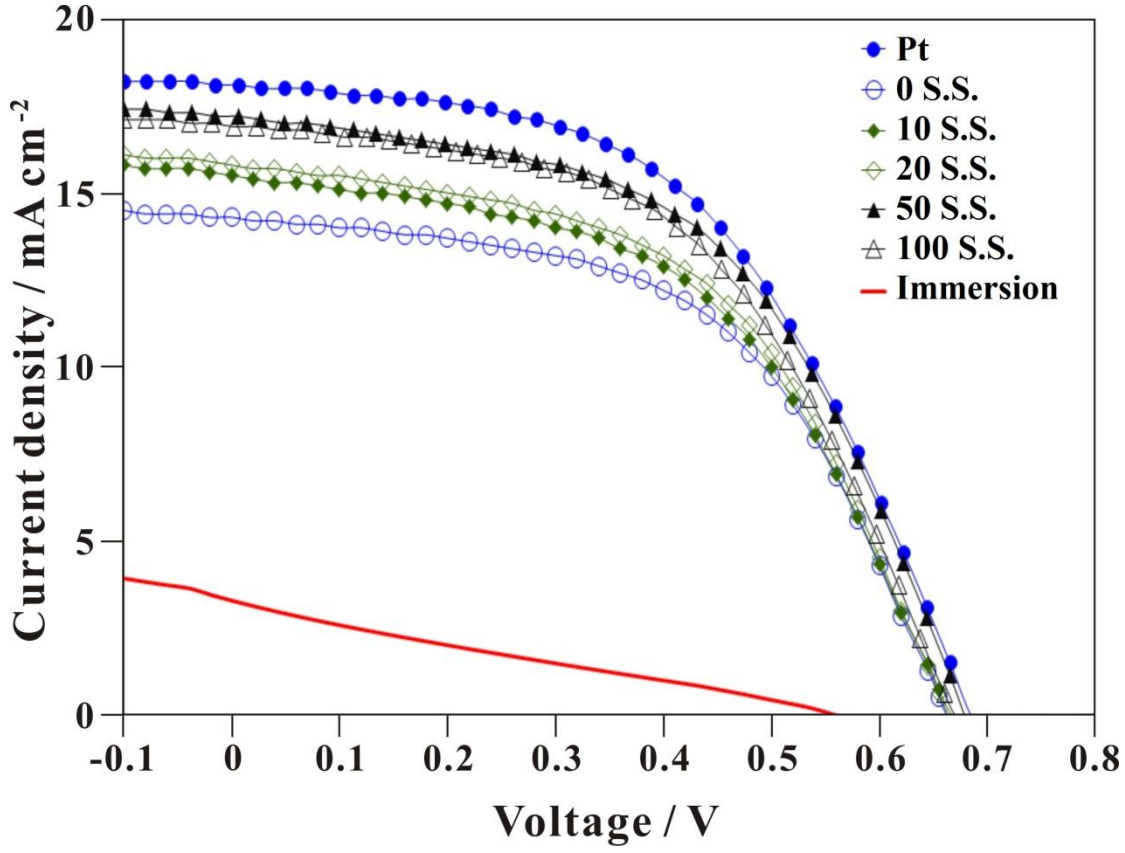


**Figure 6.** Photocurrent density-voltage curves of DSSCs based on CEs of Pt film and immersion, 0-, 10-, 20-, 50- and 100-sweep-segment (S.S.) iodine films on PEDOT/ITO, respectively. The measurements were recorded under 100 mW $cm^{-2}$, AM 1.5.

These findings demonstrate that two inverse effects should be given by the film that increased the active interface and electronic transport resistance in the film. The decrease in interfacial charge transfer resistance (Fig. 7) and the increase in peak current density (Fig. 5) were predominantly correlated with an augmented active interface with increasing thickness (Fig. 2 and Table 1). The increase in electronic transport resistance in the film decreased the electrode reaction rate and accelerated electronic recombination in the DSSC [35], inducing decreases in solar cells photovoltaic performance for the 100-sweep-segment electrodes.

### *3.4. Photoelectric performances of DSSCs*

Fig. 6 showed photovoltaic performances of DSSCs with different electrodeposition times of iodine thickness, measured at 100 mW $cm^{-2}$ light intensity and illuminated from the CE side.

**Table 2.** The photovoltaic parameters of DSSCs based on CEs of different sweep segments iodine film on PEDOT/ITO.

| Iodine film (swee segments) | $J_{sc}$ (mA $cm^{-2}$) | $V_{oc}$ (V) | FF (%) | η (%) | $R_{ct1}$ (Ω) | $R_{ct2}$ (Ω) |
|---|---|---|---|---|---|---|
| 0 | 14.28 | 0.673 | 52.77 | 5.07 | 8.94 | 8.82 |
| 10 | 15.49 | 0.680 | 50.17 | 5.28 | 9.15 | 8.39 |
| 20 | 15.80 | 0.676 | 51.03 | 5.54 | 6.58 | 9.27 |
| 50 | 17.19 | 0.679 | 51.88 | 6.06 | 6.18 | 10.55 |
| 100 | 16.94 | 0.676 | 51.07 | 5.84 | 22.32 | 7.47 |

Table 2 showed the corresponding open-circuit voltage ($V_{oc}$), short-circuit current density ($J_{sc}$), fill factor (FF) and cell efficiency (η) for DSSCs with different iodine electrodeposition times. The $J_{sc}$ value increased with the iodine film thickness up to 50-sweep-segment and decreased at 100-sweep-segment. Form 50- to 100-sweep-segments, the gradually decrease of $J_{sc}$ may be attributed to the decrease in transmittance with the increase of iodine thickness. When the iodine film thickness increased to 100-sweep-segment, the cell performance was decreased. The best cell efficiency of 6.06% was achieved at the iodine film thickness of 50-sweep-segment.

### *3.5. AC impedance spectra of DSSCs*

EIS technique was used to study the charge transfer resistances of the cells, which were in consistency with the results obtained from the photovoltaic characteristic. Fig. 7 illustrated the EIS data of the solar cells base on different iodine film thickness (sweep-segments) on PEDOT/ITO. The ohmic serial resistance ($R_s$) in the equivalent circuit corresponds to the overall series resistance. In general, the impedance spectrum of a DSSC showed three semicircles in the frequency range of 100 mHz to 1 MHz. The first, second and third semicircles correspond to the charge transfer resistances at

the CE ($R_{ct1}$), at the $TiO_2$/dye/electrolyte interface ($R_{ct2}$) and to the Warburg diffusion process of $I^-/I_3^-$ in the electrolyte ($R_{diff}$), respectively. A very thin spacer was used in our device. Therefore, the $R_{diff}$ was not obvious, and it was overlapped by $R_{ct2}$.

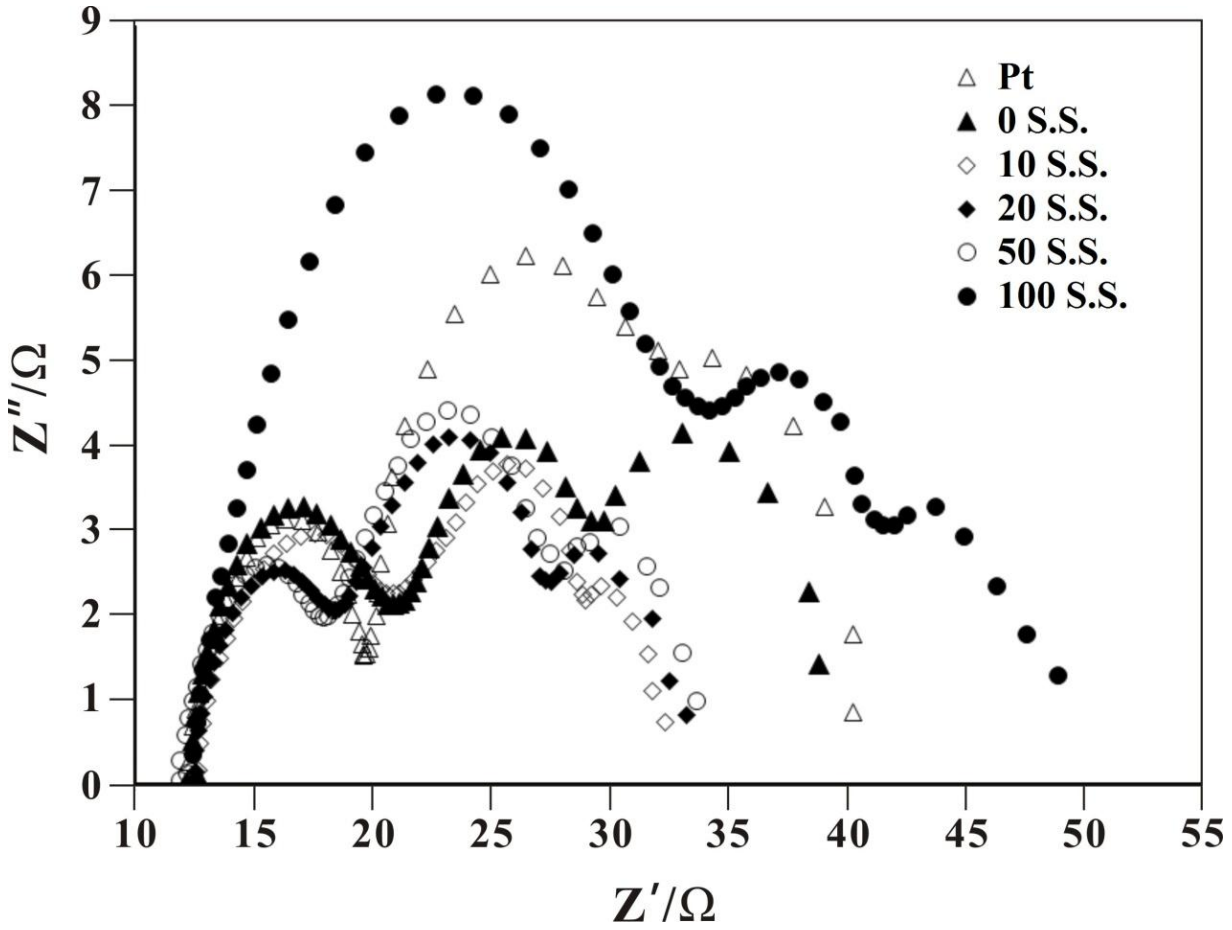


**Figure 7.** AC impedance spectra of DSSCs based on CEs of Pt film and immersion, 0-, 10-, 20-, 50- and 100-sweep-segment (S.S.) iodine films on PEDOT/ITO, respectively. The measurements were recorded under 100 mW $cm^{-2}$, AM 1.5.

The corresponding values of $R_{ct1}$ and $R_{ct2}$ were shown in Table 2. The lower $R_{ct1}$ values with the increase of iodine film thickness up to 50-sweep-segment due to the higher catalytic ability of the iodine-PEODT film, but decreased at the 100-sweep-segment. The above result indicated the iodine film thickness of 50-sweep-segment on PEDOT/ITO is the optimal condition for DSSC.

## 4. CONCLUSION

Various iodine films on PEDOT/ITO CEs for DSSCs were successfully demonstrated as a means of increasing the efficiency of DSSC. The information of various iodine films were monitored by CV, AC impedance, UV-vis spectroscopy, SEM and AFM. It is confirmed that the optimal

thickness of iodine film on PEDOT/ITO is 50-sweep-segment for high-performance DSSCs and showed a 19.5% improvement of conversion efficiency under full sunlight of 100 mW $cm^{-2}$ (AM 1.5) conditions.

ACKNOWLEDGMENT
This work was supported by the National Science Council of Taiwan.

**References**

1. B. O'Regan, M. Gratzel, *Nature* 353 (1991) 737.
2. A.Kay, M. Gratzel, *Sol. Energy Mater. Sol. Cells* 44 (1996) 99.
3. M. H. Lai, M. W. Lee, Gou-Jen Wang and M. F. Tai, *Int. J. Electrochem. Sci*., 6 (2011) 2122 – 2130.
4. B. O'Regan, M. Gratzel, *Nature* 353 (1991) 737.
5. N.G. Park, K.M. Kim, M.G. Kang, K.S. Ryu, S.H. Chang, Y.J. Shin, *Adv. Mater*. 17 (2005) 2349.
6. K. Lee, S.W. Park, M.J. Ko, K. Kim, N.-G. Park, *Nat. Mater*. 8 (2009) 665.
7. W. Lee, S.-J. Roh, K.-H. Hyung, R.S. Mane, S.-H. Lee, S.-H. Han, *Sol. Energy* 83 (2009) 690.
8. R. Jose, V. Thavasi, S. Ramakrishna, J. *Am. Ceram. Soc*. 92 (2009) 289.
9. A.Mishra, M.K.R. Fischer, P. Bauerle, *Angew Chem. Int*. Ed. 48 (2009) 2474.
10. S.J. Lim, Y.S. Kang, D.-W. Kim, *Electrochem. Commun*. 12 (2010) 1037.
11. C.H. Yoon, R. Vittal, J. Lee, W.-S. Chae, K.-J. Kim, *Electrochim. Acta* 53 (2008) 2890.
12. T.N. Murakami, M. Grätzel, *Inorganica Chim. Acta* 361 (2008) 572.
13. Kuo-Chiang Lin, Tsung-Hsuan Tsai, Shen-Ming Chen, *Biosensors and Bioelectronics* 26 (2010) 608-614.
14. Tsung-Hsuan Tsai, Tse-Wei Chen, Shen-Ming Chen, *Electroanalysis* 22 (2010) 1655–1662.
15. G. Inzelt, M. Pineri, J. W. Schultze, M. A. Vorotyntsev, *Electrochim. Acta* 2000, 45, 2403.
16. Tse-Wei Chen, Tsung-Hsuan Tsai, Shen-Ming Chen, Kuo-Chiang Lin, *Int. J. Electrochem. Sci*., 6 (2011) 2043–2057.
17. E. M. Genies, A. Boyle, M. Lapkowski, C. Tsintavis, *Synth. Met.* 1990, 36, 139.
18. Tsung-Hsuan Tsai, Kuo-Chiang Lin, Shen-Ming Chen, *Int. J. Electrochem. Sci*., 6 (2011) 2672–2687.
19. Tsung-Hsuan Tsai, Tse-Wei Chen, Shen-Ming Chen, Kuo-Chiang Lin, *Int. J. Electrochem. Sci*., 6 (2011) 2058–2071.
20. V. S. Vasantha, S. M. Chen, *Electrochim. Acta* 2005, *51*, 347.
21. V. S. Vasantha, S. M. Chen, *J. Electroanal. Chem.* 2006, *592*, 77.
22. W. Hong, Y. Xu, G. Lu, C. Li and G. Shi, *Electrochemistry Communications*, 10 (2008) 1555.
23. Jun Zhang, Xiaoxue Li, Wei Guo, Tubshin Hreid, Jinfeng Hou, Haiquan Su, Zhuobin Yuan, *Electrochimica Acta* 56 (2011) 3147–3152.
24. E.M.J. Johansson, A. Sandell, H. Siegbahn, H. Rensmo, B. Mahrov, G. Boschloo, E. Figgemeier, A. Hagfeldt, S.K.M. Jönsson, M. Fahlman, *Synthetic Metals*, 149 (2005) 157-167.
25. Jian-Ging Chen, Hung-Yu Wei, Kuo-Chuan Ho, *Solar Energy Materials and Solar Cells*, 91 (2007) 1472-1477.
26. P. Balraju, Manish Kumar, M.S. Roy, G.D. Sharma, *Synthetic Metals*, 159 (2009) 1325-1331.
27. Chao-Ching Chang, Ming-Tai Jiang, Chen-Liang Chang, Cheng-Lan Lin, *Materials Chemistry and Physics*, 127 (2011) 440-445.
28. H. Tang, A. Kitani, M. Shionani, *J. Appl. Electrochem*. 26 (1996) 36.
29. S. Biallozor, A. Kupniewska, *Electrochem. Commun*. 2 (2000) 480.
30. X. Huang, Y.X. Li, Y.L. Chen, L. Wang, *Sens. Actuators* B 134 (2008) 780.

31. M.R. Miah, T. Ohsaka, *Anal. Chem*. 78 (2006) 1200.
32. D. Nematollahi, M. Hesari, *J. Anal. Chem*. 56 (2001) 1109.
33. D. Nematollahi, M. Hesari, *Microchemical J.* 70 (2001) 7.
34. L. Fotouhi, M. Ganjavi, D. Nematollahi, *Sensors* 4170 (2004) 180.
35. J. Zhang, T. Hreid, X. Li, W. Guo, L. Wang, X. Shi, H. Su and Z. Yuan, *Electrochimica Acta*, 55 (2010) 3664.
36. Chun-Chen Yang, Huan Qing Zhang, Yu Rong Zheng, *Current Applied Physics* 11 (2011) S147-S153.